AMERICAN SOCIETY FOR MICROBIOLOGY | mSphere®

RESEARCH ARTICLE

Neutralizing *Staphylococcus aureus* Virulence with AZD6389, a Three mAb Combination, Accelerates Closure of a Diabetic Polymicrobial Wound

Christine Tkaczyk,[a] Omari Jones-Nelson,[a]* Yue Yue Shi,[a]§ David E. Tabor,[a] Lily Cheng,[b] Tianhui Zhang,[c] Bret R. Sellman[a]

[a]Early Vaccines and Immune Therapies, BioPharmaceuticals R&D, AstraZeneca, Gaithersburg, Maryland, USA
[b]Oncology Safety, Clinical Pharmacology and Safety Sciences, R&D, AstraZeneca, Gaithersburg, Maryland, USA
[c]Data Sciences and Quantitative Biology AstraZeneca, Gaithersburg, Maryland, USA

ABSTRACT Nonhealing diabetic foot ulcers (DFU), a major complication of diabetes, are associated with high morbidity and mortality despite current standard of care. Since *Staphylococcus aureus* is the most common pathogen isolated from nonhealing and infected DFU, we hypothesized that *S. aureus* virulence factors would damage tissue, promote immune evasion and alter the microbiome, leading to bacterial persistence and delayed wound healing. In a diabetic mouse polymicrobial wound model with *S. aureus*, *Pseudomonas aeruginosa*, and *Streptococcus pyogenes*, we report a rapid bacterial proliferation, prolonged pro-inflammatory response and large necrotic lesions unclosed for up to 40 days. Treatment with AZD6389, a three-monoclonal antibody combination targeting *S. aureus* alpha toxin, 4 secreted leukotoxins, and fibrinogen binding cell-surface adhesin clumping factor A resulted in full skin re-epithelization 21 days after inoculation. By neutralizing multiple virulence factors, AZD6389 effectively blocked bacterial agglutination and *S. aureus*-mediated cell killing, abrogated *S. aureus*-mediated immune evasion and targeted the bacteria for opsonophagocytic killing. Neutralizing *S. aureus* virulence not only facilitated *S. aureus* clearance in lesions, but also reduced *S. pyogenes* and *P. aeruginosa* numbers, damaging inflammatory mediators and markers for neutrophil extracellular trap formation 14 days post initiation. Collectively, our data suggest that AZD6389 holds promise as an immunotherapeutic approach against DFU complications.

IMPORTANCE Diabetic foot ulcers (DFU) represent a major complication of diabetes and are associated with poor quality of life and increased morbidity and mortality despite standard of care. They have a complex pathogenesis starting with superficial skin lesions, which often progress to deeper tissue structures up to the bone and ultimately require limb amputation. The skin microbiome of diabetic patients has emerged as having an impact on DFU occurrence and chronicity. DFU are mostly polymicrobial, and the Gram-positive bacterium *Staphylococcus aureus* detected in more than 95% of cases. *S. aureus* possess a collection of virulence factors which participate in disease progression and may facilitate growth of other pathogens. Here we show in a diabetic mouse wound model that targeting some specific *S. aureus* virulence factors with a multimechanistic antibody combination accelerated wound closure and promoted full skin re-epithelization. This work opens promising new avenues for the treatment of DFU.

KEYWORDS Staphylococcus aureus, alpha toxin, clumping factor A, diabetic foot, leukocidins, monoclonal antibodies, polymicrobial infections, wound healing

The incidence of diabetes has increased dramatically over the past two decades, affecting more than 10% of the population worldwide (1). Diabetes is associated with a high morbidity and mortality, and diabetic foot ulcers (DFU) are a major complication of the disease with ~$13 billion annual cost to the health care system in the United

Editor Paul D. Fey, University of Nebraska Medical Center

Address correspondence to Christine Tkaczyk, christine.tkaczyk@astrazeneca.com.

*Present address: Omari Jones-Nelsona, Toeroek Associates, Lorton, Virginia, USA.

§Present address: Yue Yue Shi, Regeneron Pharmaceuticals, Tarrytown, New York, USA.

The authors declare a conflict of interest. This work was funded by AstraZeneca. C.T., L.C., D.E.T., T.Z., and B.R.S. are employees of AstraZeneca and may hold AstraZeneca stock. O.N.J. and Y.Y.S. were employees of AstraZeneca and may hold AstraZeneca stock.

Received 8 March 2022
Accepted 27 April 2022
Published 1 June 2022

States alone (2). Defects in lower extremity blood flow, neuropathy, poor glycemic control and an abnormal host immune response are associated with delayed healing, chronic wounds and recurrence (3, 4). DFU pathophysiology is complex (5) and current standard of care (SOC) relies on wound debridement, management of infection, revascularization procedures when required and off-loading of the ulcer along with appropriate glycemic control (6, 7). However, recurrence rates and severe complications indicate these approaches are not sufficient to achieve complete wound re-epithelization and prevent recurrence (5). To address this unmet medical need, several experimental molecules or approaches are currently under clinical evaluation to improve upon SOC. This includes topical administration of growth factors, *in situ* gene therapy with vascular endothelial growth factor (VEGF) or hepatocyte growth factor (HGF) (reviewed in Ref. 8), a wound dressing containing metalloproteinase inhibitors (9) or topical oxygen therapy (10). To date, only topical platelet derived growth factor (PDGF) has been approved by the FDA but may only be used for neuropathic ulcers with adequate peripheral circulation (11).

The skin microbiome has emerged as playing an integral role in DFU occurrence and healing (12–14). All DFU are colonized with microorganisms, but only ~50% are considered infected based on presence of clinical signs such as redness, purulence, swelling, warmth, pain, or induration (5, 15). Microbiological analysis of these foot ulcers by 16S rRNA sequencing demonstrated that DFU are polymicrobial, with *Staphylococcus aureus* being the most commonly identified pathogen in western countries and its presence was linked to nonhealing ulcers (6, 15–17). Other bacteria, such as *P. aeruginosa* and *S. pyogenes* are frequently detected along with *S. aureus* (18–21).

S. aureus is a Gram-positive opportunistic pathogen that causes a variety of infections, including surgical site infections, skin and soft tissue infections, bacteremia, and pneumonia (22) and can exhibit resistance to available antibiotic therapy. Consequently, alternative approaches to antibacterial therapy are being explored such as immunotherapy with specific monoclonal antibodies (MAbs) (23–25). *S. aureus* differentially expresses a variety of virulence factors in response to its environment and stage of infection to modify and evade a protective host immune response (26, 27). Among those, *S. aureus* secretes several pore-forming toxins including alpha toxin (AT) and the bicomponent leukotoxins (Leuk) which together lyse immune cells, induce a strong pro-inflammatory response and promote bacterial dissemination by damaging tissue and increasing vascular permeability (28, 29). Additionally, the *S. aureus* genome harbors a collection of microbial surface components recognizing adhesive matrix molecules (MSCRAMMs) which facilitate bacterial attachment to exposed extracellular matrix molecules leading to bacterial agglutination, biofilm formation and immune evasion (30). Therefore, we hypothesized that some *S. aureus* virulence factors would promote DFU colonization and create a local environment permissive for pathogen outgrowth resulting in chronic, nonhealing wounds. To determine if targeting *S. aureus* was beneficial in the healing process and could accelerate wound closure, we developed a polymicrobial wound model in diabetic mice with *S. aureus* and two other pathogens, *P. aeruginosa* and *S. pyogenes*, and tested the efficacy of anti-*S. aureus* AZD6389 MAb combination. These last two organisms were selected based on their prevalence in polymicrobial DFU along with *S. aureus*, and as primary causes of infection and delayed wound healing (31–34). AZD6389, a multimechanistic combination of three MAbs, targets *S. aureus* virulence factors AT, 4 bicomponent leukotoxins (LukSF/LukED/HlgAB/HlgCB) and the fibrinogen binding surface expressed MSCRAMM, clumping factor A (ClfA). These MAbs were identified for their ability to respectively inhibit *in vitro* AT-hemolytic activity (35), leukotoxins cytolytic activity, ClfA-mediated blood agglutination and bacteria opsonophagocytic killing (25). Together, this combination provides broad strain coverage in multiple *S. aureus* disease models (25, 36, 37). We found that diabetic animals challenged with a mixture of *S. aureus*/*S. pyogenes*/*P. aeruginosa* developed large, unhealed lesions resulting in part from bacterial proliferation, sustained local inflammation and neutrophil extracellular trap (NET) formation. AZD6389 administration accelerated bacterial clearance, decreased inflammation and reduced markers of NET formation leading to more rapid wound closure. Together, our results demonstrated that *S. aureus* virulence factors act in concert to create

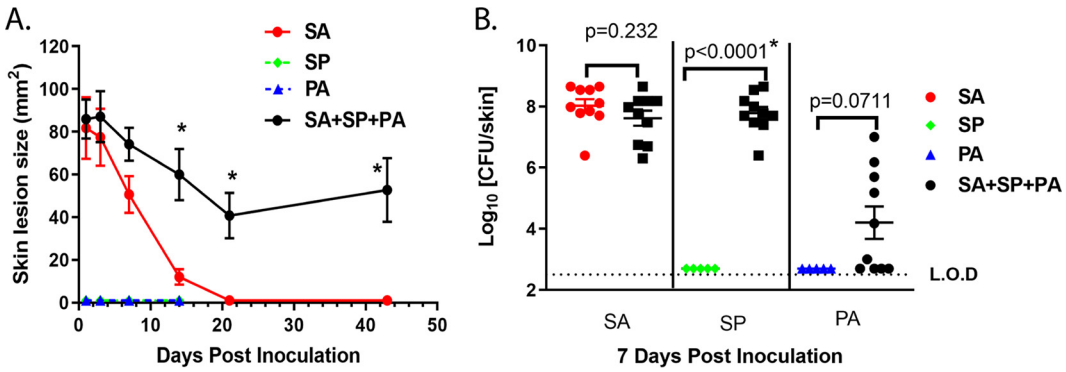

FIG 1 *S. aureus* (SA), *P. aeruginosa* (PA) and *S. pyogenes* (SP) mixed infection in the diabetic polymicrobial wound. (A) Skin lesion sizes induced by ID injection of SA SF8300 (1.0×10^7 CFU), SP (10 CFU), PA (1.0×10^5 CFU) or SA/SP/PA ($n = 10$ per group). Lesions were measured at indicated times and graphed as mean values ± standard error of the mean (SEM). Statistical significance for lesion sizes between two groups was determined using a Vardi's AUC test (two sample tests for growth under the curve dependent right censoring) and considered statistically different if $P < 0.05$. PA vs SA $P = 0.012$; PA vs SA/PA/SP $P = 0.0036$; SA vs SA+SP+PA $P = 0.005$; SA vs SP $P = 0.0012$; SP vs SA+PA+SP $P = 0.0036$ (B) *S. aureus*, *S. pyogenes* and *P. aeruginosa* recovered from skin lesions of mice injected as described above after 7 days. Significant difference for CFU was analyzed with a Mann-Whitney test, and considered statistically different if $P < 0.05$ as indicated with a (*).

an environment permissive to pathogen outgrowth and promote the persistence of a chronic wound. Targeting *S. aureus* with the AZD6389 may open new avenues for the treatment of DFU.

RESULTS

Diabetic mice fail to heal wounds after polymicrobial inoculation. *S. aureus* is highly prevalent in DFU and is frequently present with other pathogens including *S. pyogenes* and *P. aeruginosa* (12, 38, 39). To better understand polymicrobial DFU pathogenesis and to determine if targeting *S. aureus* with pathogen specific MAbs could promote wound healing in a polymicrobial setting, we developed a wound model in db/db$^{-/-}$ type 2 diabetic mice with a mixture of *S. aureus*, *P. aeruginosa* and *S. pyogenes*. In a first attempt, intradermal (i.d.) inoculation with 1.0×10^5 CFU (CFU) *P. aeruginosa* and *S. pyogenes* combined with 1.0×10^7 SA resulted in large lesions (>400 mm^2) 7 days postinoculation (Fig. S1 in the supplemental material), which were much larger than wounds resulting from the i.d. inoculation of one or two pathogens. These results indicated that polymicrobial infection was more severe than individual infections, but the inoculum of bacteria used was too rapidly progressive for a diabetic wound since mice succumbed from infection after 7 days (Fig. S1A). To reduce the disease severity of the three-pathogen mixture and replicate the chronic nature of a diabetic wound, the bacterial CFU were titrated down, and the model ultimately established with 1.0×10^7 *S. aureus*, 1.0×10^5 *P. aeruginosa*, and 1.0×10^1 *S. pyogenes*. Although *S. aureus*/*P. aeruginosa*/*S. pyogenes* mixture- or *S. aureus*-injected mice exhibited similar skin lesion sizes (~100 mm^2) 24 h postinoculation, *S. aureus*-induced lesions fully healed within 3 weeks while the mice injected with three bacteria mixture developed a wound that did not heal for up to 6 weeks (Fig. 1A). Additionally, inoculation with *S. aureus*/*P. aeruginosa*/*S. pyogenes* resulted in > 6 log outgrowth of *S. pyogenes* on day 7 relative to *S. pyogenes* injected alone ($P = 0.0007$). While not statistically significant, a similar 4 log increase in *P. aeruginosa* was observed relative to *P. aeruginosa* alone ($P = 0.0711$); however *S. aureus* CFU were similar in mice injected with *S. aureus* alone or *S. aureus*/*P. aeruginosa*/*S. pyogenes* (Fig. 1B). Nondiabetic lean mice (db/db$^{-/+}$) inoculated with *S. aureus*/*S. pyogenes*/*P. aeruginosa* developed significantly smaller lesions compared to diabetic littermates ($P = 0.0002$) (Fig. 2A and B). Bacterial growth in nondiabetic mice was also significantly reduced for *S. aureus* and *S. pyogenes* on day 14 ($P < 0.05$, Fig. 2C), and the bacteria were no longer detectable after 21 days (Fig. 2C). These results suggest that in a diabetic host, a mixed skin infection potentiates bacterial growth and prevents healing compared to infection with individual pathogens.

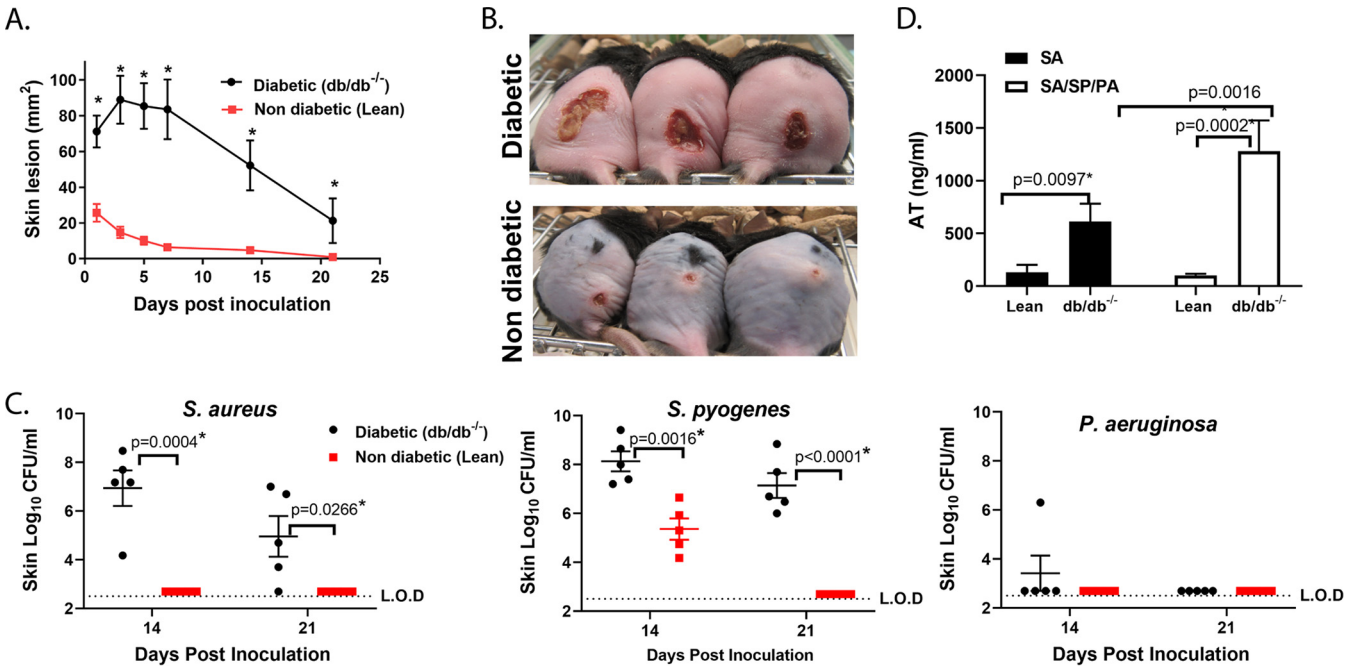

FIG 2 Polymicrobial wound healing and bacterial clearance is delayed in diabetic mice. (A) Skin lesion sizes of diabetic and nondiabetic mice (n = 10 per group) i.d. injected with *S. aureus* SF8300 (SA) - (1.0×10^7 CFU)/*P. aeruginosa* (PA) (1.0×10^5 CFU)/*S. pyogenes* (SP) (10 CFU). Lesions were measured at indicated times and graphed as mean values ± SEM. Statistical significance for lesion sizes between diabetic and nondiabetic mice injected with *S. aureus*/*S. pyogenes*/*P. aeruginosa* was determined using a Vardi's AUC test (two sample tests for growth under the curve dependent right censoring) and considered statistically different if $P < 0.05$ as indicated with a (*). (B) Pictures of representative skin lesions 14 days after i.d. inoculation. (C) *S. aureus*, *S. pyogenes* and *P. aeruginosa* recovered from skin lesions after 14 or 21 days from mice inoculated as indicated in (A). Data are represented at mean values ± SEM. Statistical difference for CFU was analyzed with a Mann-Whitney test, and considered statistically different if $P < 0.05$ as indicated with a (*). (D) Skins was harvested 24 h postchallenge with *S. aureus* or *S. aureus*/*S. pyogenes*/*P. aeruginosa*, homogenized and analyzed by ELISA for AT content (ng/mL). Statistical difference between group was analyzed with a Mann-Whitney t test, and considered statistically different if $P < 0.05$.

S. aureus AT has been reported to potentiate bacterial growth and increase disease severity in a mouse mixed bacterial lung infection model (40). AT is also reported to be a key virulence factor in *S. aureus*-skin and soft tissue infection models and could play a similar role in the diabetic polymicrobial wound model (23, 41, 42). Here, AT levels in skin lesions 24h post-injection of *S. aureus* alone were significantly higher in diabetic animals compared to lean littermates (Fig. 2D and $P = 0.0097$) and this difference was even more pronounced in the mixed polymicrobial wound (Fig. 2D $P = 0.0002$, and Fig. S2 for multiple *S. aureus* clinical wound isolates). Collectively, these data demonstrate that AT expression is potentiated in diabetic mice and even more so in a polymicrobial wound, suggesting it may play a role in the delayed wound healing seen in this polymicrobial wound model, but the complex nature and multiple stages of a DFU may require targeting different aspects of *S. aureus* virulence.

Targeting *S. aureus* virulence factors with a specific MAb combination accelerates healing. DFU pathogenesis is complex and can represent different diseases starting with a superficial skin lesion progressing into deeper tissue and even into the bone which can lead to bloodstream infections and amputation (43). To target a single pathogen like *S. aureus* with a MAb-based approach, we hypothesized it would require multiple antibodies to neutralize different virulence factors to provide broad disease coverage and *S. aureus* isolate coverage in a complex disease such as DFU. We previously demonstrated that the administration of an α-AT and α-ClfA MAb combination was required to provide broad disease coverage in multiple *S. aureus*-induced preclinical models (25, 44). More recently, AZD6389 comprised of MEDI4893* (α-AT), AZD7745 (α-ClfA) and the anti-leukotoxin MAb AZD8887 (α-Leuk) demonstrated efficacy in mouse and rabbit surgical models (36, 37). We therefore tested whether targeting *S. aureus* with the multimechanistic MAb combination AZD6389 (described in Fig. S3 in the supplemental material) provided benefit in the diabetic polymicrobial wound

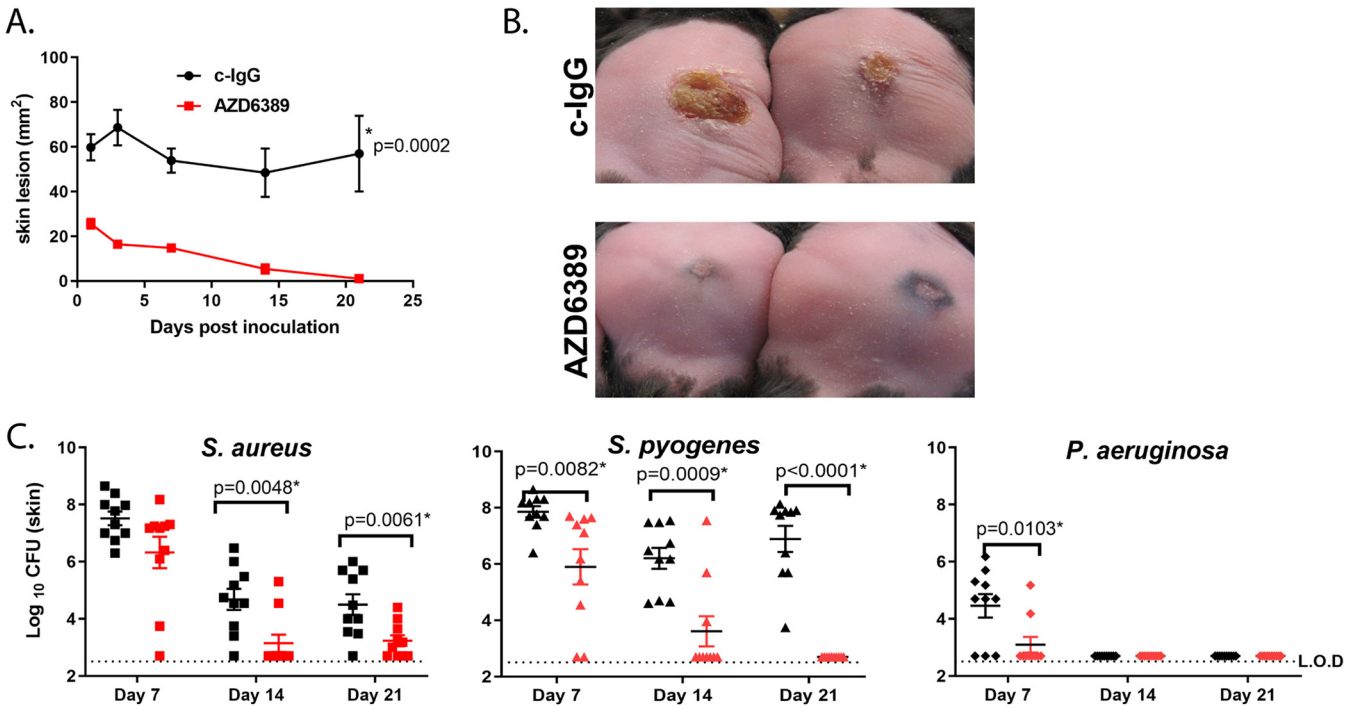

FIG 3 Targeting a single pathogen with AZD6389 accelerates polymicrobial wound closure. Diabetic mice (n = 10 per group) were passively immunized with AZD6389 (15 mg/kg each MAb) or c-IgG (15 mg/kg) and challenged 24 h later with *S. aureus* SF8300 (1.0×10^7 CFU)/*P. aeruginosa* (1.0×10^5 CFU)/*S. pyogenes* (10 CFU). (A) Skin lesion sizes were measured at indicated times and graphed as mean values ± SEM. Statistical difference between c-IgG and AZD6389 group was determined using a Vardi's AUC test (two sample tests for growth under the curve dependent right censoring) and considered statistically different if $P < 0.05$ as indicated with a (*). (B) Representative pictures of skin lesions 21 days after challenge. (C) Bacteria CFU in lesions at indicated times postchallenge. Data represent mean values ± standard deviation (error bars). Statistical difference for CFU between both group was analyzed with a Mann-Whitney test, and considered statistically different if $P < 0.05$ as indicated with a (*).

model. Passive immunization with AZD6389 24 h prior to inoculation with a *S. aureus*/*P. aeruginosa*/*S. pyogenes* mixture resulted in full wound closure within 21 days, while wounds in mice that received a negative control IgG (c-IgG) remained unhealed out to 21 days (Fig. 1A and Fig. 3A). Moreover, neutralizing *S. aureus* virulence enabled the immune system to clear *S. aureus* and impaired *S. aureus*-mediated outgrowth of *S. pyogenes* and *P. aeruginosa* (Fig. 3C).

All three MAb components of AZD6389 are required for wound closure in therapy. To determine if AZD6389 could provide a therapeutic benefit, the MAb combination was administered before or at different times after initiation of the polymicrobial wound. AZD6389 injection up to 8 h after inoculation accelerated closure of wounds initiated with different *S. aureus* wound isolates (Table S1 in the supplemental material) combined with *S. pyogenes*/*P. aeruginosa* in the polymicrobial wound model (Fig. S4 and Fig. 4). In this model, mice received 15 mg/kg of each anti-*S. aureus* MAb or 15 mg/kg of c-IgG. However, since no significant difference in kinetic of wound closure between c-IgG at 15 or 45 mg/kg groups were observed when administered in prophylaxis or 8 h postinoculation (Fig. S5A and Fig. S5B), c-IgG was used at 15 mg/kg for the study. To better understand the contribution and requirement of each MAb in wound healing, mice were treated with either the individual MAbs, a combination of two MAbs (α-AT+ α-ClfA, α-AT+ α-Leuk, or α-ClfA+ α-Leuk) or the three MAb combination AZD6389, 8 h post polymicrobial inoculation. Treatment with the combination of all three MAbs resulted in accelerated wound closure. In contrast, treatment with either the individual MAbs, the combination of two MAbs or c-IgG did not result in complete wound closure by day 21 (Fig. 5 and Fig. S6). These results demonstrate that all three MAbs are required to accelerate wound closure in diabetic mice. Histopathological examination of the skin after H&E staining demonstrated that AZD6389 treatment resulted in full closure after 21 days as shown by complete full-thickness re-epithelization and fewer

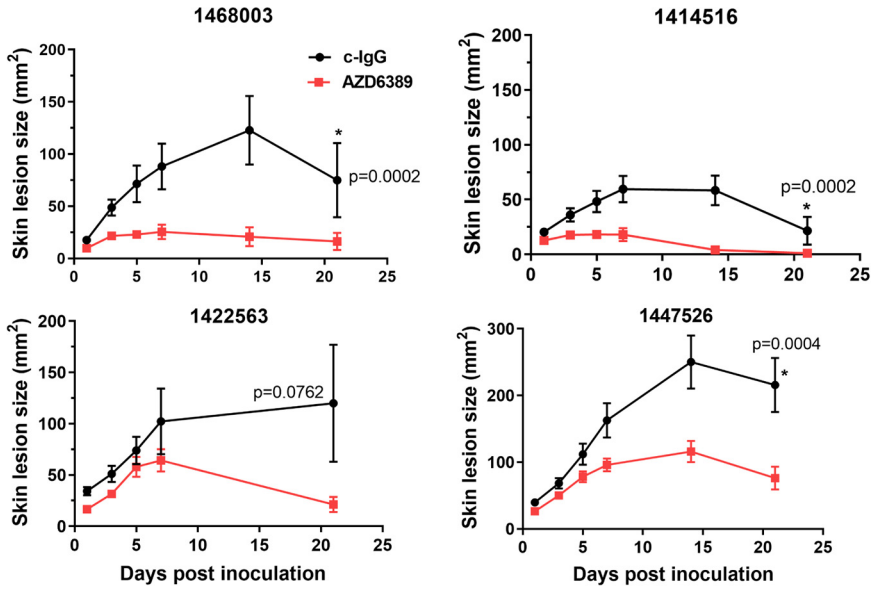

FIG 4 AZD6389 provides *S. aureus* strain coverage in the diabetic polymicrobial wound. Skin lesion size of mice (n = 10) inoculated with *S. pyogenes* (10 CFU)/*P. aeruginosa* (1.0×10^5 CFU) and various *S. aureus* wound isolates (1.0×10^6 CFU). AZD6389 (15 mg/kg each MAb) or c-IgG (15 mg/kg) was administered i.p 8 h later, and then 7 days later. Skin lesion sizes were measured at indicated days and represented as mean values ± standard errors mean (error bars). Statistical analysis between c-IgG and AZD6389 group was determined for each strain using a Vardi's AUC test (two sample tests for growth under the curve dependent right censoring), and considered statistically different ($P < 0.05$) as indicated with a (*).

inflammatory cells compared with skin from mice treated with c-IgG (Fig. 6 and Table S2). The effect of the anti-*S. aureus* MAb combination on bacterial CFU was quantified by measuring CFU 14 days after inoculation. AZD6389 significantly decreased *S. aureus* CFU (P = 0.0042) as well as *S. pyogenes* (P= 0.0137) and *P. aeruginosa* (P = 0.0054) compared to c-IgG (Fig. S7).

AZD6389 reduced immune defects in diabetic wounds. Wound healing is a complex process involving coagulation, inflammation, cell proliferation and tissue remodeling (45). Diabetes is associated with immune defects including inflammatory dysregulation (46) and neutrophil activation (47, 48), which may delay the wound healing process. To determine the effect of AZD6389 on some aspects of the immune response, pro-inflammatory mediators were quantified in the skin lesions. Pro-inflammatory cytokines and matrix metalloproteinase 9 (MMP-9) were significantly decreased by the MAb combination compared to c-IgG 7 days postinoculation, with a more pronounced effect after 14 days for TNF-α and IFN-γ, suggesting that AZD6389 alleviated some of the prolonged pro-inflammatory response observed in the diabetic polymicrobial wound (Fig. 7A and B). Another hypothesis for delayed wound healing in diabetics is the propensity of neutrophils to form extra-cellular traps or NETs (49). Enzymatic activity of PAD_4, a molecule controlling an intracellular pathway initiating NETosis along with neutrophil elastase (NE) and myeloperoxidase (MPO), two prototypical NET markers, were increased in the c-IgG treated mice over time and decreased in mice treated with AZD6389 (Fig. 7C). Together, these data demonstrated that neutralizing *S. aureus* virulence diminished the pro-inflammatory environment associated with nonhealing diabetic wounds.

DISCUSSION

Microbial colonization, biofilm formation and infection are important factors linked to delayed healing of a diabetic foot ulcer (DFU) (12, 33, 50). DFU pathogenesis is complex and cover a broad range of diseases (43). Most DFUs are colonized with numerous bacteria (51), but *S. aureus* presence is associated with delayed healing and worse disease outcomes (52, 53). *S. aureus* possesses a large collection of virulence factors involved in skin and

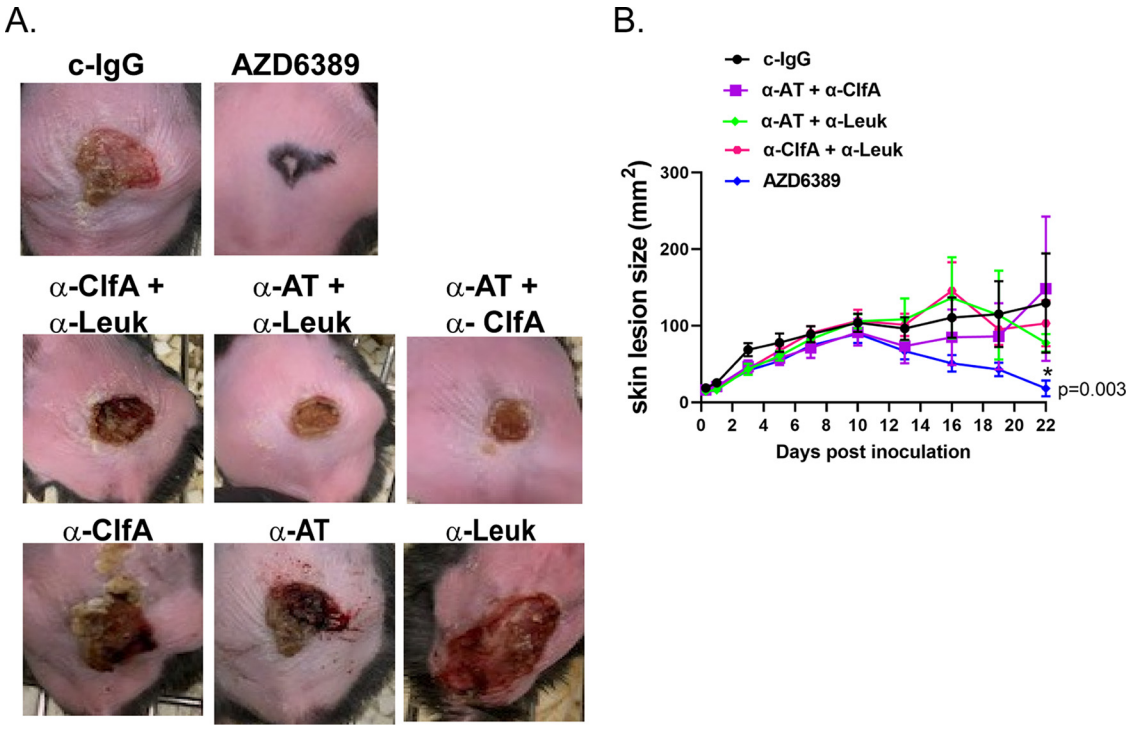

FIG 5 All three components of AZD6389 are required for closure of the polymicrobial wound. Diabetic mice (n = 10 per group) were inoculated with *S. aureus* 1447526 (1.0×10^6 CFU)/*P. aeruginosa* (1.0×10^5 CFU)/*S. pyogenes* (10 CFU), and i.p. immunized 8 h later with c-IgG, duo MAb combination or AZD6389 trio MAbs (all MAbs at 15 mg/kg). Animals were immunized 7 days later with same MAb combinations (A) Representative pictures of wounds 21 days postinoculation. (B) Kinetic of wound closure (lesion sizes) for c-IgG, duo combinations and AZD6389 treated groups. Lesion sizes were recorded at indicated times and represented as mean values ± standard errors (error bars). Statistical analysis between c-IgG and each group was determined using a Vardi's AUC test (two sample tests for growth under the curve dependent right censoring), and considered statistically different ($P < 0.05$) as indicated with a (*).

wound colonization, and can promote tissue damage, biofilm formation and disease progression (54). However, bacterial interactions and their role in nonhealing DFU are poorly understood. Here we demonstrate that i.d. inoculation of diabetic mice with three bacterial pathogens results in more severe wounds than inoculation with one or two pathogens and that targeting multiple *S. aureus* virulence factors (AT, the bicomponent leukotoxins, and ClfA) with AZD6389 accelerated wound healing in mice with polymicrobial wounds.

AT and the four bicomponent leukotoxins LukSF/LukED/HlgAB/HlgCB are pore forming toxins with a broad cell tropism that damage tissue and enable the bacteria to evade the host immune system (28, 55). Since *P. aeruginosa* has been reported to increase AT production in *S. aureus*/*P. aeruginosa* coinfected pig skin (56) and AT neutralization accelerates wound closure of *S. aureus* infected wounds in diabetic mice (57), we speculated that persistence in our polymicrobial diabetic wound was due in part to increased AT levels. We found that *S. aureus* expresses higher AT levels in diabetic mice than in nondiabetic littermates (Fig. 2), and even more in the presence of *P. aeruginosa* and *S. pyogenes* in the diabetic wounds (Fig. S2 in the supplemental material). We previously reported that *S. aureus* potentiated a mixed bacterial lung infection and promoted pathogen outgrowth in part through AT mediated impairment of alveolar macrophage phagocytic activity (40). AT may have a similar effect in the current model however, therapeutic administration of α-AT MAb MEDI4893 was not sufficient to promote wound healing, suggesting that other virulence factors are also involved in delayed healing in diabetic mice (Fig. 5 and Fig. S6).

Bacterial communities in chronic wounds form biofilms and downregulate genes involved in proliferation, resulting in reduced susceptibility to phagocytic killing and antibiotics (50). *S. aureus* biofilm formation may increase in a diabetic host since it exploits the hypercoagulable state in diabetics by upregulating surface expression of

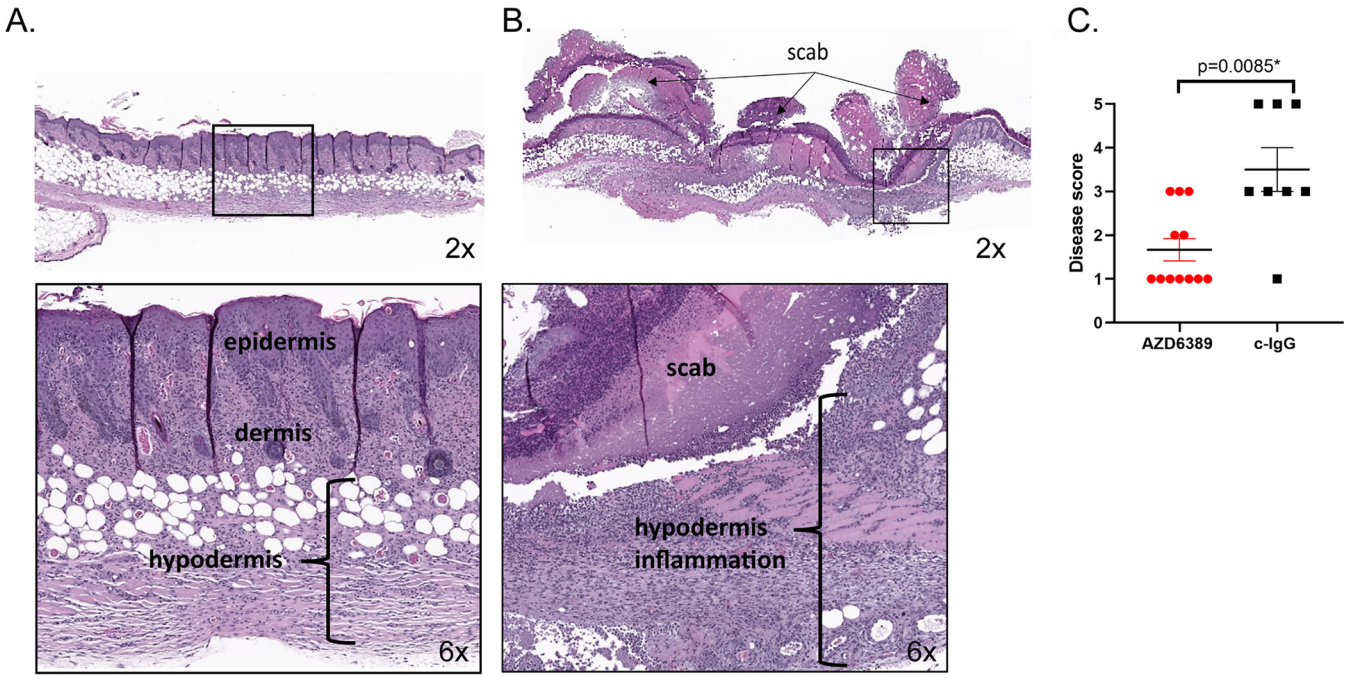

FIG 6 AZD6389 therapy provides full skin re-epithelization in the diabetic polymicrobial wound. Representative histology from mice (n = 12-8) inoculated i.d. with *S. aureus* 1447526 (1.0×10^6 CFU)/*P. aeruginosa* (1.0×10^5 CFU)/*S. pyogenes* (10 CFU). AZD6389 (15 mg/kg for each MAb) or c-IgG (15 mg/kg) were administered i.p. 8 h later, and then 7 days later. Each skin lesion was stained with H&E 21 days postinoculation. (A) Representative skin of AZD6389 treated mice showed epidermal closure (top left, 2X), with minimal inflammation and proliferation of fibroblast within the dermis and hypodermis (bottom left, 6X). (B) Representative skin of mice treated with c-IgG showed marked necrotic lesion under a serocellular scab (top right, magnification $\times$2) with full thickness inflammation, and necrotic cellular debris admixed with blood and bacterial colonies (bottom right, 6X). (C) Skin disease scoring (n = 12-8) $\pm$SEM.

ClfA (58), a fibrinogen-binding adhesin essential for bacterial agglutination, biofilm and abscess formation as well as inhibition of complement-mediated phagocytosis (30). We recently demonstrated the complementary roles of AT and ClfA in the mouse hematogenous implant-related *S. aureus* biofilm infection model and determined that targeting both AT and ClfA (with MEDI4893 and AZD7745) provided benefit over the individual MAbs, highlighting the need for a MAb combination (36, 44). In a lethal mouse bacteremia model, we have demonstrated that the anti-AT/Anti-ClfA MAb combination required both the anti-ClfA human MAb opsonophagocytic killing activity and ability to prevent agglutination for protection (59). Wozniak et al. also showed that *S. aureus* biofilms released the LukSF and HlgAB leukotoxins to elicit NET formation and escape neutrophil-mediated phagocytosis (60). This may explain why only AZD6389, a multimechanistic MAb combination comprising an α-Leuk MAb combined with α-AT and α-ClfA MAbs which to-

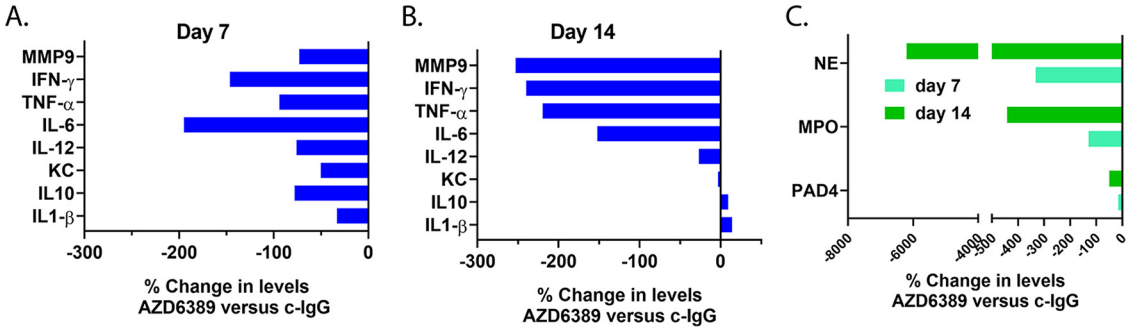

FIG 7 AZD6389 reduces the prolonged pro-inflammatory phase in the polymicrobial diabetic wound. Mice (n = 10) were inoculated i.d. with *S. aureus* 1447526 (1.0×10^6 CFU)/*P. aeruginosa* (1.0×10^5 CFU)/*S. pyogenes* (10 CFU). MAbs (15 mg/kg for each MAb) was administered i.p. 8 h later, and then 7 days later. Skin lesions were harvested at day 7 or 14 postinoculation, homogenized and homogenates analyzed for cytokines or metalloproteinase contents (A and B) or markers for NET formation (B). Data were normalized as % of change in levels for AZD6389 treated mice versus c-IgG.

gether inhibits bacterial agglutination, cell lysis and promotes opsonophagocytic killing (Fig. S3), was required for complete skin re-epithelization in a *S. aureus*/*S. pyogenes*/*P. aeruginosa* -inoculated diabetic wounds.

Functional defects of neutrophils (49) and macrophages (61) in diabetic individuals are associated with tissue damage and delayed wound healing. *S. aureus* secreted enzymes such as hyaluronidase (62) increases permeability of connective tissues and may amplify these defects by facilitating neutrophil and macrophage recruitment in the wound. Diabetes is associated with low grade inflammation which primes neutrophils for spontaneous NETosis (3, 46). It has been reported that AT stimulates NET formation by a low density neutrophil population enriched in diabetic animals (63). NETosis is also increased by TNF-α (46), a cytokine elevated and sustained in the polymicrobial wound (Fig. 7A and B). Therefore, by neutralizing AT and the leukotoxins and decreasing pro-inflammatory cytokines present in the polymicrobial wound microenvironment, AZD6389 reduced markers of NET formation as evidenced by decreases in PAD_4, MPO, and NE (Fig. 7C).

Targeting *S. aureus* with a multimechanistic MAb combination provides several benefits. *S. aureus* expression of secreted toxins and ClfA dependent of the specific strain and their lifestyle and growth phase (27). By neutralizing multiple virulence factors AZD6389 could extend coverage throughout the different stages of DFU pathogenesis. In fact, the multimechanistic MAb combination and its component MAbs have been reported to provide protection in a variety of disease models that may represent different aspects of DFU pathogenesis as it progresses from a superficial wound into deeper tissues including the bone and in some case resulting in systemic bloodstream infections. These models include dermonecrosis, surgical wound infection, a bone implant infection and bacteremia in addition to the diabetic polymicrobial wound model reported here (23, 25, 36, 37, 44, 57). Together, the results reported herein support a role for *S. aureus* in the development of chronic polymicrobial diabetic wounds and specifically targeting *S. aureus* virulence with the multimechanistic MAb combination AZD6389 may open new therapeutic perspectives for all stages of DFU.

MATERIALS AND METHODS

Bacteria strains and growth. Community-acquired methicillin-resistant *S. aureus* (CA-MRSA) USA300 SF8300 strain was previously described (59). Clinical *S. aureus* wound isolates 1414516, 1422563, 1447526, 1468003 were obtained from a collection of an international antibiotic resistance surveillance program. Basic demographic data (age, sex, hospital location, sample type) were provided for each isolate by International Health Management Associates (IHMA). Beta hemolytic *S. pyogenes* strain BAA-947 strain Rosenbach was purchased from ATCC (Manassas, VA). *P. aeruginosa* cytotoxic strain 6077 was provided by J. B. Goldberg (University of Virginia, Charlottesville, VA). Bacteria were grown to mid-log phase at an optical density at 600 nm (OD_{600}) of 0.8 in Trypticase soy broth (TSB, VWR International), washed twice in ice cold PBS (Invitrogen), and frozen in 10% glycerol-TSB aliquots. *S. aureus* and *S. pyogenes* challenge inocula were prepared from one frozen vial for each experiment, diluted in ice-cold PBS pH 7.2 (VWR International), and placed on ice until injection. *P. aeruginosa* was streaked on a Tryptic soy agar (TSA) plate (VWR International), incubated overnight at 37°C and the challenge inoculum was prepared by diluting one single colony in PBS to 1×10^5 CFU/mL.

Whole-genome sequencing and genetic analysis. DNA was purified from bacterial cultures via bead beating followed by extraction using a PureLink Genomic DNA minikit (ThermoFisher). Sequencing libraries were prepared by Covaris mechanical shearing followed by a NEBNext Ultra DNA library preparation kit for Illumina (New England BioLabs Inc.). Sequencing was performed via MiSeq 2×250 runs (Illumina) with a targeted depth of 150-fold. Multi-Locus Sequence Typing was performed by SRST2 (64) using a *S. aureus* MLST database downloaded from pubmlst.org on 08OCT2021. Read sets were screened for leukotoxins by direct-read mapping implemented in SRST2 (64), using a 90% coverage cut-off and reference genes obtained from USA300_FPR3757 GenBank: CP000255.1. Sequences were assembled *de novo* with SPAdes (65) and annotated with Prokka (66). Agr typing was performed by BLAST (67) of isolate agrC genes against representative agrC genes from each agr type: agr type I GenBank: AF210055; agr type II GenBank: AF001782; agr type III GenBank: AF001783; and agr type IV GenBank: AF288215 (68).

Monoclonal antibodies and reagents. All MAbs are human IgG1 isotype. Anti-AT (α-AT) MAb MEDI4893 (or LC10) and anti-clumping factor A (α-ClfA) MAb AZD7745 (or SAR114) were previously described (24, 25) Cross-neutralizing leukotoxin (anti-LukSF/LukED/HlgAB/HlgCB or α-Leuk) AZD8887 (SAN481) MAb was generated by Humabs (Bellinzona, Switzerland) through Antigen-specific Memory B cell Repertoire Analysis (AMBRA) technology as previously described (36). Anti-gp120 human IgG1 R347 MAb was used as negative control (23) and indicated as c-IgG.

Mice. All animal studies were approved by the AstraZeneca Institutional Animal Care and Use Committee, and they were conducted in an Association for Accreditation and Assessment Laboratory Animal Care (AAALAC)-accredited facility in compliance with U.S. regulations governing the housing and use of animals. Eight- to 9-week-old male diabetic mice (glucose level ≥500 mg/dL) of strain BKS.Cg-Dock7m Leprdb/+ +/J were purchased from Jackson Laboratories (Bar Harbor, Maine) developed spontaneously clinical sign with similar features than human type 2 diabetes. Age matched male nondiabetic C57BLKS/J animals were used as lean control. BKS.Cg-Dock7m Leprdb/+ -/J were used as lean controls.

Polymicrobial wound Model. Mice were shaved and treated with Nair on their back (VWR International**)** 48 h prior bacterial inoculation. Animals were intradermal (i.d.) injected with 50 μL of bacteria mixture prepared as described above and monitored daily for any sign of distress. Mice were immunized with MAbs intraperitoneal (i.p.), diluted in 500 μL of cold PBS, either prophylactically 24 h before inoculation therapeutically at different times post i.d. challenge.

Skin lesion sizes were recorded at indicated time points on each figure and lesion area calculated as described previously (23). Statistical analysis between groups were performed for corrected repeated measures. For each animal, area under the curve (AUC) was calculated, and comparison of AUC were performed between groups using a Vardi's AUC test (Two-sample tests for growth curves under dependent right censoring) (69). Difference between groups for kinetic of skin lesion sizes were considered statistically different if $P < 0.05$ and indicated with a (*).

All experiments were performed in accordance with institutional guidelines following experimental protocol review and approval by the Institutional Biosafety Committee (IBC) and the Institutional Animal Care and Use Committee (IACUC) at AstraZeneca.

Bacteria enumeration. Animals were euthanized at indicated times following bacteria ID challenge, and bacteria CFU were quantified from total skin lesions. Skins were placed in sterile tubes containing 1 mL cold PBS and processed with a homogenizer (Omni Prep multisample homogenizer; Omni International, Marietta, GA). Bacteria were then serially diluted and CFU for *S. aureus*, *S. pyogenes* and *P. aeruginosa* determined respectively after plating on TSA, Blood agar, and Orientation CHROMagar plates (Becton, Dickinson). The limit of detection for bacteria enumeration in our model was 200 CFU.

Mediator quantification in skin lesions. Skin lesions were harvested at the indicated times postinoculation and processed as in (23) for protein extraction. Pro-inflammatory cytokines were measured with an Mesoscale 9-Plex pro-inflammatory mouse cytokines kit (Mesoscale, Gaithersburg, MD). Matrix metallo-proteinase 9 (MMP9) was measured with an enzyme-linked immune-absorbent assay (ELISA) kit (R&D systems). Myeloperoxidase (MPO), neutrophil elastase (NE) and PAD_4 were quantified with assay kits from Cayman Chemical (Ann Harbor, MI). Values were normalized to pg/mg skin and expressed as % change in levels for AZD6389-treated group versus c-IgG group.

Histology. Mice were euthanized at indicated time postinoculation and skin lesions harvested, fixed in buffered 10% formalin (VWR International) for 24 h, and paraffin embedded (Leica Microsystems). Four μm sections were stained with hematoxylin and eosin (H&E, Mercedes Medical) following standard histopathological techniques. Stained slides were digitally scanned on Aperio AT2 slide scanner (Leica BioSystems) at ×20 magnification and photomicrographs were taken at 2× and 6× magnifications. All stained sections were analyzed using a Nikon 90i brightfield microscope by a blinded board-certified pathologist and scored from 0 (*normal*) to 5 (*severe*).

Quantification of alpha toxin in skin lesions. Skin lesions were harvested with an 8-mm wound punch after 1 or 5 days of bacteria inoculation, and snap-frozen on liquid nitrogen. Skins were processed for protein extraction as detailed in (23). AT in lesions was quantified by ELISA. Maxisorp 96-well plates (Nunc) were coated with purified anti-AT MAb MEDI4893* (0.1 μg/mL) in 100 μL of 0.2M carbonate/bicarbonate buffer, and incubated overnight at 4°C. After three washes with PBS 0.1% Tween (wash buffer), plates were blocked at room temperature with 200 μL of PBS 2%BSA (Sigma). Following three washes, twofold serial dilutions in PBS (starting at 1:2) of digested skin supernatants were added to the plates under 50 μL and incubated for 90 min at room temperature with a 200 rpm orbital shaking. Purified AT was used as a standard (twofold serial dilutions starting at 200 ng/mL). After three washes, plates were incubated with polyclonal rabbit IgG anti-AT (2 μg/mL) in 50 μL PBS 0.1%BSA for 1 h at room temperature with a 200 rpm shaking. Following three washes, 50 μL of HRP-conjugated goat anti-rabbit IgG was added to the plates for 30 min at room temperature. After final washes, 100 μL of TMB substrate (KPL) was added, and the reaction was stopped after 8 min with 100 μL 0.2 M H_2SO_4. The optical density at 450 nm was measured with a spectrophotometer (Molecular Devices). AT quantity was expressed in ng/mL.

Leukotoxin cytolytic assay on human neutrophils. Human neutrophils were purified from heparin-drawn blood of three healthy anonymous volunteers (AstraZeneca employee blood donor program, male and female), as previously described (40). In a flat bottom white 96-well plate (Greiner), 25 μL of twofold serial dilution of anti-leukotoxin MAb AZD8887 or trio MAb AZD6389 were incubated for 15 min at room temperature with 25 μL of leukotoxin giving 90% of cell lysis, respectively of LukSF (200 ng/mL), LukED (4000 ng/mL), HlgAB (2000 ng/mL) or HlgCB (200 ng/mL).Plate was incubated for 2 h in a 37°C incubator with 5% CO_2 after adding 50 μL of purified neutrophils to each well., followed by addition of 100 μL of Cell Titer Glo (Promega). After 30 min of shaking at 200 rpm, luminescent signal in relative luminescent unit (RLU) was measured with an Envision Multilabel plate reader (Perkin Elmer). Percentage of cell viability was calculated as follows: $100 - \{100 * [(RLU_{toxin\ +\ mAb})/(RLU_{cells\ alone})]\}$.

Alpha toxin (AT) hemolytic assay on rabbit red blood cells. Rabbit red blood cell (RBC) hemolytic assay was performed as described previously (25). Briefly, serial dilutions of anti-AT MAb MEDI4893* or trio MAb AZD6389 (500 to 1.7 nM) were mixed with AT (0.1 μg/mL = 3 nM) in a U bottom 96-well plate (Thermo Fisher Scientific) and incubated with 50 μL of washed rabbit RBC (Peel Freeze) for 1 h at 37°C. Plates then were centrifuged at 1200 rpm for 3 min, and 50 μL of supernatant was transferred to new

plates. Nonspecific human IgG1 R347 was used as a negative control (c-IgG). The optical density at 450 nm (OD_{450})was measured with a spectrophotometer (Molecular Devices). Percentage of inhibition of hemolysis was calculated as follow: 100 − [100* ($OD_{AT\ +\ MAb}$/$OD_{AT,\ no\ MAb}$)].

Opsonophagocytic killing assay. HL-60 cells were obtained from ATCC (Manassas, VA). HL-60 cells were cultured and differentiated as described (25). Cells were washed in saline and adjusted to 1.0 × 10^7 cells/mL in high-glucose Hanks balance salt solution (HG-HBSS) (Invitrogen) with 0.1% gelatin (Sigma). Human serum collected from a healthy volunteer (AstraZeneca employee blood donor program) was adsorbed against *S. aureus* Reynolds capsule type 5 and *S. aureus* Wright capsule type 8 to deplete endogenous *S. aureus*-specific IgG and used as a complement source (1:100). USA300 SF8300 CA-MRSA clinical isolate was grown overnight in TSB, washed in cold saline, and diluted to 1e6 CFU/mL in saline. 10 μL of bacteria was incubated on ice for 30 min with 10 μL of anti-ClfA MAb AZD7745 or AZD6389 trio MAb serial dilution in 60 μL of HG-HBSS 0.1% gelatin. Ten microliters of sera and 10 μL of HL-60 were then added to the opsonized bacteria. Ten microliters of samples from each well were serially diluted in water with 0.1% saponin and dropped on a TSA plate (VWR International) before and after incubation for 1 h at 37°C with 100 rpm orbital shaking. Bacterial colonies were counted after 16 h of incubation of TSA plates at 37°C. The percentage of OPK was calculated as follows: 100 − [100* ($CFU_{at\ 1\ h}$)/($CFU_{at\ time\ zero}$)].

Fibrinogen-ClfA binding assay. Nunc MaxiSorp plates (Thermo Fisher Scientific) were coated overnight at 4°C with 2 μg/mL human fibrinogen (Sigma), washed with PBS containing 0.1% Tween 20 (wash buffer), and blocked for 1 h at room temperature (RT) with 200 μL/well casein (Thermo Fisher). Following three washes, the plates were incubated for 1 h at room temperature with a mix of 50 μL AviTag ClfA221–559 (2 μg/mL) and serial dilutions of anti-ClfA MAb AZD7745* or trio MAb AZD6389 in a 100 μL final volume of PBS. After three washes, bound ClfA was detected using horseradish peroxidase (HRP)-conjugated streptavidin (1:20,000; GE Healthcare) and then 100 μL of 3,3′,5,5′-tetramethylbenzidine (TMB) substrate (KPL). The reaction was stopped after 10 min with 100 μL 0.2 M H_2SO_4. The optical density at 450 nm (OD_{450}) was measured with a spectrophotometer (Molecular Devices). The percent inhibition of ClfA binding to fibrinogen was calculated as follow: 100 − [100 * ($OD_{ClfA+MAb}$/$OD_{ClfA,no\ MAb}$)].

Agglutination assay in human sera. *S. aureus* clinical isolates were cultured overnight in 10 mL of TSB, washed in PBS, and suspended in 1 mL of ice-cold PBS. Anti-ClfA MAb AZD7745 or trio MAb AZD6389 were twofold serially diluted in 30 μL PBS starting at 200 μg/mL and mixed with 30 μL of citrated human plasma (AstraZeneca employee blood donor program) in a 96-well U-bottom plate (Thermo Fisher Scientific). Bacteria were added (30 μL) and incubated for 5 min at 37°C. Each well was evaluated visually, and the lowest MAb concentration where bacteria agglutinated was recorded. R347 was utilized as an isotype control human IgG1 (c-IgG).

Statistics. Statistical difference analysis was performed using Prism v9 (GraphPad). Data are represented as means standard errors of the mean (SEM), and values of $P < 0.05$ were considered to be statistically significant.

SUPPLEMENTAL MATERIAL

Supplemental material is available online only.

FIG S1, TIF file, 0.1 MB.

FIG S2, TIF file, 0.1 MB.

FIG S3, TIF file, 0.1 MB.

FIG S4, TIF file, 0.1 MB.

FIG S5, TIF file, 0.1 MB.

FIG S6, TIF file, 0.1 MB.

FIG S7, TIF file, 0.1 MB.

TABLE S1, TIF file, 0.1 MB.

ACKNOWLEDGMENTS

This work was funded by AstraZeneca. C.T., L.C., D.E.T., T.Z., and B.R.S. are employees of AstraZeneca and may hold AstraZeneca stock. O.N.J. and Y.Y.S. were employees of AstraZeneca and may hold AstraZeneca stock.

C.T. designed the study, analyzed data and wrote the manuscript. O.N.J., Y.Y.S. designed, researched and analyzed data. T.Z. and L.C. analyzed the data, B.R.S. reviewed and edited the manuscript, and contributed to the discussion. C.T. is the guarantor of this work, and had full access to all the data of the study and takes responsibility for the integrity of the data and the accuracy of the data analysis.

REFERENCES

1. WHO. 2016. Global Report in Diabetes. World Health Organization, Geneva.
2. Rice JB, Desai U, Cummings AK, Birnbaum HG, Skornicki M, Parsons NB. 2014. Burden of diabetic foot ulcers for medicare and private insurers. Diabetes Care 37:651–658. https://doi.org/10.2337/dc13-2176.
3. Wong SL, Demers M, Martinod K, Gallant M, Wang Y, Goldfine AB, Kahn CR, Wagner DD. 2015. Diabetes primes neutrophils to undergo NETosis, which impairs wound healing. Nat Med 21:815–819. https://doi.org/10.1038/nm.3887.

4. Li G, Zou X, Zhu Y, Zhang J, Zhou L, Wang D, Li B, Chen Z. 2017. Expression and influence of matrix metalloproteinase-9/tissue inhibitor of metalloproteinase-1 and vascular endothelial growth factor in diabetic foot ulcers. Int J Low Extrem Wounds 16:6–13. https://doi.org/10.1177/1534734617696728.
5. Armstrong DG, Boulton AJM, Bus SA. 2017. Diabetic foot ulcers and their recurrence. N Engl J Med 376:2367–2375. https://doi.org/10.1056/NEJMra1615439.
6. Lipsky BA, Silverman MH, Joseph WS. 2017. A proposed new classification of skin and soft tissue infections modeled on the subset of diabetic foot infection. Open Forum Infect Dis 4:ofw255. https://doi.org/10.1093/ofid/ofw255.
7. Armstrong DG, Lavery LA, Harkless LB. 1998. Validation of a diabetic wound classification system: The contribution of depth, infection, and ischemia to risk of amputation. Diabetes Care 21:855–859. https://doi.org/10.2337/diacare.21.5.855.
8. Ohnstedt E, Lofton Tomenius H, Vagesjo E, Phillipson M. 2019. The discovery and development of topical medicines for wound healing. Expert Opin Drug Discov 14:485–497. https://doi.org/10.1080/17460441.2019.1588879.
9. Edmonds M, Lazaro-Martinez JL, Alfayate-Garcia JM, Martini J, Petit JM, Rayman G, Lobmann R, Uccioli L, Sauvadet A, Bohbot S, Kerihuel JC, Piaggesi A. 2018. Sucrose octasulfate dressing versus control dressing in patients with neuroischaemic diabetic foot ulcers (Explorer): an international, multicentre, double-blind, randomised, controlled trial. Lancet Diabetes Endocrinol 6:186–196. https://doi.org/10.1016/S2213-8587(17)30438-2.
10. Frykberg RG, Franks PJ, Edmonds M, Brantley JN, Teot L, Wild T, Garoufalis MG, Lee AM, Thompson JA, Reach G, Dove CR, Lachgar K, Grotemeyer D, Renton SC, Group TWOS. 2020. A multinational, multicenter, randomized, double-blinded, placebo-controlled trial to evaluate the efficacy of cyclical topical wound oxygen (TWO2) therapy in the treatment of chronic diabetic foot ulcers: The TWO2 Study. Diabetes Care 43:616–624. https://doi.org/10.2337/dc19-0476.
11. Papanas N, Maltezos E. 2008. Becaplermin gel in the treatment of diabetic neuropathic foot ulcers. Clin Interv Aging 3:233–240. https://doi.org/10.2147/cia.s1106.
12. Gardner SE, Frantz RA. 2008. Wound bioburden and infection-related complications in diabetic foot ulcers. Biol Res Nurs 10:44–53. https://doi.org/10.1177/1099800408319056.
13. Bowler PG. 2018. Antibiotic resistance and biofilm tolerance: a combined threat in the treatment of chronic infections. J Wound Care 27:273–277. https://doi.org/10.12968/jowc.2018.27.5.273.
14. Redel H, Gao Z, Li H, Alekseyenko AV, Zhou Y, Perez-Perez GI, Weinstock G, Sodergren E, Blaser MJ. 2013. Quantitation and composition of cutaneous microbiota in diabetic and nondiabetic men. J Infect Dis 207:1105–1114. https://doi.org/10.1093/infdis/jit005.
15. Lipsky BA, Senneville E, Abbas ZG, Aragon-Sanchez J, Diggle M, Embil JM, Kono S, Lavery LA, Malone M, van Asten SA, Urbancic-Rovan V, Peters EJG. 2020. Guidelines on the diagnosis and treatment of foot infection in persons with diabetes (IWGDF 2019 update). Diabetes Metab Res Rev 36(Suppl 1):e3280. https://doi.org/10.1002/dmrr.3280.
16. Roberts AD, Simon GL. 2012. Diabetic foot infections: the role of microbiology and antibiotic treatment. Semin Vasc Surg 25:75–81. https://doi.org/10.1053/j.semvascsurg.2012.04.010.
17. Gardner SE, Hillis SL, Heilmann K, Segre JA, Grice EA. 2013. The neuropathic diabetic foot ulcer microbiome is associated with clinical factors. Diabetes 62:923–930. https://doi.org/10.2337/db12-0771.
18. Montejo M. 2012. Daptomycin in diabetic patients. Enferm Infecc Microbiol Clin 30(Suppl 1):54–58. https://doi.org/10.1016/S0213-005X(12)70073-3.
19. Stappers MH, Hagen F, Reimnitz P, Mouton JW, Meis JF, Gyssens IC. 2015. Direct molecular versus culture-based assessment of Gram-positive cocci in biopsies of patients with major abscesses and diabetic foot infections. Eur J Clin Microbiol Infect Dis 34:1885–1892. https://doi.org/10.1007/s10096-015-2428-4.
20. Al Ayed MY, Ababneh M, Alwin Robert A, Alzaid A, Ahmed RA, Salman A, Musallam MA, Al Dawish MA. 2018. Common pathogens and antibiotic sensitivity profiles of infected diabetic foot ulcers in Saudi Arabia. Int J Low Extrem Wounds 17:161–168. https://doi.org/10.1177/1534734618793557.
21. Wolcott RD, Hanson JD, Rees EJ, Koenig LD, Phillips CD, Wolcott RA, Cox SB, White JS. 2016. Analysis of the chronic wound microbiota of 2,963 patients by 16S rDNA pyrosequencing. Wound Repair Regen 24:163–174. https://doi.org/10.1111/wrr.12370.
22. Lowy FD. 1998. *Staphylococcus aureus* infections. N Engl J Med 339:520–532. https://doi.org/10.1056/NEJM199808203390806.
23. Tkaczyk C, Hamilton MM, Datta V, Yang XP, Hilliard JJ, Stephens GL, Sadowska A, Hua L, O'Day T, Suzich J, Stover CK, Sellman BR. 2013. *Staphylococcus aureus* alpha toxin suppresses effective innate and adaptive immune responses in a murine dermonecrosis model. PLoS One 8:e75103. https://doi.org/10.1371/journal.pone.0075103.
24. Hua L, Hilliard JJ, Shi Y, Tkaczyk C, Cheng LI, Yu X, Datta V, Ren S, Feng H, Zinsou R, Keller A, O'Day T, Du Q, Cheng L, Damschroder M, Robbie G, Suzich J, Stover CK, Sellman BR. 2014. Assessment of an anti-alpha-toxin monoclonal antibody for prevention and treatment of *Staphylococcus aureus*-induced pneumonia. Antimicrob Agents Chemother 58:1108–1117. https://doi.org/10.1128/AAC.02190-13.
25. Tkaczyk C, Kasturirangan S, Minola A, Jones-Nelson O, Gunter V, Shi YY, Rosenthal K, Aleti V, Semenova E, Warrener P, Tabor D, Stover CK, Corti D, Rainey G, Sellman BR. 2017. Multimechanistic monoclonal antibodies (MAbs) targeting staphylococcus aureus alpha-toxin and clumping factor A: activity and efficacy comparisons of a mab combination and an engineered bispecific antibody approach. Antimicrob Agents Chemother 61. https://doi.org/10.1128/AAC.00629-17.
26. Thammavongsa V, Kim HK, Missiakas D, Schneewind O. 2015. Staphylococcal manipulation of host immune responses. Nat Rev Microbiol 13:529–543. https://doi.org/10.1038/nrmicro3521.
27. Jenkins A, Diep BA, Mai TT, Vo NH, Warrener P, Suzich J, Stover CK, Sellman BR. 2015. Differential expression and roles of *Staphylococcus aureus* virulence determinants during colonization and disease. mBio 6:e02272-14–e02214. https://doi.org/10.1128/mBio.02272-14.
28. Berube BJ, Bubeck Wardenburg J. 2013. *Staphylococcus aureus* alpha-toxin: nearly a century of intrigue. Toxins (Basel) 5:1140–1166. https://doi.org/10.3390/toxins5061140.
29. Alonzo F, 3rd, Torres VJ. 2014. The bicomponent pore-forming leucocidins of *Staphylococcus aureus*. Microbiol Mol Biol Rev 78:199–230. https://doi.org/10.1128/MMBR.00055-13.
30. Foster TJ, Geoghegan JA, Ganesh VK, Hook M. 2014. Adhesion, invasion and evasion: the many functions of the surface proteins of *Staphylococcus aureus*. Nat Rev Microbiol 12:49–62. https://doi.org/10.1038/nrmicro3161.
31. Gardiner M, Vicaretti M, Sparks J, Bansal S, Bush S, Liu M, Darling A, Harry E, Burke CM. 2017. A longitudinal study of the diabetic skin and wound microbiome. PeerJ 5:e3543. https://doi.org/10.7717/peerj.3543.
32. Lipsky BA, Pecoraro RE, Wheat LJ. 1990. The diabetic foot. Soft tissue and bone infection. Infect Dis Clin North Am 4:409–432. https://doi.org/10.1016/S0891-5520(20)30354-8.
33. Liu C, Ponsero AJ, Armstrong DG, Lipsky BA, Hurwitz BL. 2020. The dynamic wound microbiome. BMC Med 18:358. https://doi.org/10.1186/s12916-020-01820-6.
34. Uckay I, Gariani K, Pataky Z, Lipsky BA. 2014. Diabetic foot infections: state-of-the-art. Diabetes Obes Metab 16:305–316. https://doi.org/10.1111/dom.12190.
35. Tkaczyk C, Hua L, Varkey R, Shi Y, Dettinger L, Woods R, Barnes A, MacGill RS, Wilson S, Chowdhury P, Stover CK, Sellman BR. 2012. Identification of anti-alpha toxin monoclonal antibodies that reduce the severity of *Staphylococcus aureus* dermonecrosis and exhibit a correlation between affinity and potency. Clin Vaccine Immunol 19:377–385. https://doi.org/10.1128/CVI.05589-11.
36. Ortines RV, Wang Y, Liu H, Dikeman DA, Pinsker BL, Miller RJ, Kim SE, Ackerman NE, Rizkallah JF, Marcello LT, Cohen TS, Tkaczyk C, Sellman BR, Miller LS. 2019. Efficacy of a multimechanistic monoclonal antibody combination against *Staphylococcus aureus* surgical site infections in mice. Antimicrob Agents Chemother 63. https://doi.org/10.1128/AAC.00346-19.
37. Mao Y, Valour F, Nguyen NTQ, Doan TMN, Koelkebeck H, Richardson C, Cheng LI, Sellman BR, Tkaczyk C, Diep BA. 2021. Multimechanistic monoclonal antibody combination targeting key *Staphylococcus aureus* virulence determinants in a rabbit model of prosthetic joint infection. Antimicrob Agents Chemother 65:e0183220. https://doi.org/10.1128/AAC.01832-20.
38. Pereira SG, Moura J, Carvalho E, Empadinhas N. 2017. Microbiota of chronic diabetic wounds: ecology, impact, and potential for innovative treatment strategies. Front Microbiol 8:1791. https://doi.org/10.3389/fmicb.2017.01791.
39. Macdonald KE, Boeckh S, Stacey HJ, Jones JD. 2021. The microbiology of diabetic foot infections: a meta-analysis. BMC Infect Dis 21:770. https://doi.org/10.1186/s12879-021-06516-7.
40. Cohen TS, Hilliard JJ, Jones-Nelson O, Keller AE, O'Day T, Tkaczyk C, DiGiandomenico A, Hamilton M, Pelletier M, Wang Q, Diep BA, Le VT, Cheng L, Suzich J, Stover CK, Sellman BR. 2016. Staphylococcus aureus alpha toxin potentiates opportunistic bacterial lung infections. Sci Transl Med 8:329ra31.
41. Kennedy AD, Bubeck Wardenburg J, Gardner DJ, Long D, Whitney AR, Braughton KR, Schneewind O, DeLeo FR. 2010. Targeting of alpha-hemolysin by active or passive immunization decreases severity of USA300 skin

infection in a mouse model. J Infect Dis 202:1050–1058. https://doi.org/10.1086/656043.
42. Le VT, Tkaczyk C, Chau S, Rao RL, Dip EC, Pereira-Franchi EP, Cheng L, Lee S, Koelkebeck H, Hilliard JJ, Yu XQ, Datta V, Nguyen V, Weiss W, Prokai L, O'Day T, Stover CK, Sellman BR, Diep BA. 2016. Critical role of alpha-toxin and protective effects of its neutralization by a human antibody in acute bacterial skin and skin structure infections. Antimicrob Agents Chemother 60:5640–5648. https://doi.org/10.1128/AAC.00710-16.
43. Lipsky BA. 2016. Diabetic foot infections: Current treatment and delaying the 'post-antibiotic era'. Diabetes Metab Res Rev 32 Suppl 1:246–253. https://doi.org/10.1002/dmrr.2739.
44. Wang Y, Cheng LI, Helfer DR, Ashbaugh AG, Miller RJ, Tzomides AJ, Thompson JM, Ortines RV, Tsai AS, Liu H, Dillen CA, Archer NK, Cohen TS, Tkaczyk C, Stover CK, Sellman BR, Miller LS. 2017. Mouse model of hematogenous implant-related *Staphylococcus aureus* biofilm infection reveals therapeutic targets. Proc Natl Acad Sci U S A 114:E5094–E5102. https://doi.org/10.1073/pnas.1703427114.
45. Eming SA, Martin P, Tomic-Canic M. 2014. Wound repair and regeneration: mechanisms, signaling, and translation. Sci Transl Med 6:265sr6. https://doi.org/10.1126/scitranslmed.3009337.
46. Alexandraki KI, Piperi C, Ziakas PD, Apostolopoulos NV, Makrilakis K, Syriou V, Diamanti-Kandarakis E, Kaltsas G, Kalofoutis A. 2008. Cytokine secretion in long-standing diabetes mellitus type 1 and 2: associations with low-grade systemic inflammation. J Clin Immunol 28:314–321. https://doi.org/10.1007/s10875-007-9164-1.
47. Karima M, Kantarci A, Ohira T, Hasturk H, Jones VL, Nam BH, Malabanan A, Trackman PC, Badwey JA, Van Dyke TE. 2005. Enhanced superoxide release and elevated protein kinase C activity in neutrophils from diabetic patients: association with periodontitis. J Leukoc Biol 78:862–870. https://doi.org/10.1189/jlb.1004583.
48. Hanses F, Park S, Rich J, Lee JC. 2011. Reduced neutrophil apoptosis in diabetic mice during staphylococcal infection leads to prolonged Tnfalpha production and reduced neutrophil clearance. PLoS One 6:e23633. https://doi.org/10.1371/journal.pone.0023633.
49. Fadini GP, Menegazzo L, Rigato M, Scattolini V, Poncina N, Bruttocao A, Ciciliot S, Mammano F, Ciubotaru CD, Brocco E, Marescotti MC, Cappellari R, Arrigoni G, Millioni R, Vigili de Kreutzenberg S, Albiero M, Avogaro A. 2016. NETosis delays diabetic wound healing in mice and humans. Diabetes 65:1061–1071. https://doi.org/10.2337/db15-0863.
50. Buch PJ, Chai Y, Goluch ED. 2019. Treating polymicrobial infections in chronic diabetic wounds. Clin Microbiol Rev 32. https://doi.org/10.1128/CMR.00091-18.
51. Bowler PG, Duerden BI, Armstrong DG. 2001. Wound microbiology and associated approaches to wound management. Clin Microbiol Rev 14:244–269. https://doi.org/10.1128/CMR.14.2.244-269.2001.
52. Kalan LR, Meisel JS, Loesche MA, Horwinski J, Soaita I, Chen X, Uberoi A, Gardner SE, Grice EA. 2019. Strain- and species-level variation in the microbiome of diabetic wounds is associated with clinical outcomes and therapeutic efficacy. Cell Host Microbe 25:641–655.e5. https://doi.org/10.1016/j.chom.2019.03.006.
53. Lipsky BA, Richard JL, Lavigne JP. 2013. Diabetic foot ulcer microbiome: one small step for molecular microbiology . . . one giant leap for understanding diabetic foot ulcers? Diabetes 62:679–681. https://doi.org/10.2337/db12-1325.
54. Dunyach-Remy C, Ngba Essebe C, Sotto A, Lavigne JP. 2016. *Staphylococcus aureus* toxins and diabetic foot ulcers: role in pathogenesis and interest in diagnosis. Toxins 8:209. https://doi.org/10.3390/toxins8070209.
55. Spaan AN, van Strijp JAG, Torres VJ. 2017. Leukocidins: staphylococcal bicomponent pore-forming toxins find their receptors. Nat Rev Microbiol 15:435–447. https://doi.org/10.1038/nrmicro.2017.27.
56. Pastar I, Nusbaum AG, Gil J, Patel SB, Chen J, Valdes J, Stojadinovic O, Plano LR, Tomic-Canic M, Davis SC. 2013. Interactions of methicillin resistant Staphylococcus aureus USA300 and Pseudomonas aeruginosa in polymicrobial wound infection. PLoS One 8:e56846. https://doi.org/10.1371/journal.pone.0056846.
57. Ortines RV, Liu H, Cheng LI, Cohen TS, Lawlor H, Gami A, Wang Y, Dillen CA, Archer NK, Miller RJ, Ashbaugh AG, Pinsker BL, Marchitto MC, Tkaczyk C, Stover CK, Sellman BR, Miller LS. 2018. Neutralizing alpha-toxin accelerates healing of *Staphylococcus aureus*-infected wounds in nondiabetic and diabetic mice. Antimicrob Agents Chemother 62. https://doi.org/10.1128/AAC.02288-17.
58. Farnsworth CW, Schott EM, Jensen SE, Zukoski J, Benvie AM, Refaai MA, Kates SL, Schwarz EM, Zuscik MJ, Gill SR, Mooney RA. 2017. Adaptive upregulation of clumping factor A (ClfA) by *Staphylococcus aureus* in the obese, type 2 diabetic host mediates increased virulence. Infect Immun 85. https://doi.org/10.1128/IAI.01005-16.
59. Tkaczyk C, Hamilton MM, Sadowska A, Shi Y, Chang CS, Chowdhury P, Buonapane R, Xiao X, Warrener P, Mediavilla J, Kreiswirth B, Suzich J, Stover CK, Sellman BR. 2016. Targeting alpha toxin and ClfA with a multimechanistic monoclonal-antibody-based approach for prophylaxis of serious *Staphylococcus aureus* disease. mBio 7. https://doi.org/10.1128/mBio.00528-16.
60. Bhattacharya M, Berends ETM, Chan R, Schwab E, Roy S, Sen CK, Torres VJ, Wozniak DJ. 2018. *Staphylococcus aureus* biofilms release leukocidins to elicit extracellular trap formation and evade neutrophil-mediated killing. Proc Natl Acad Sci U S A 115:7416–7421. https://doi.org/10.1073/pnas.1721949115.
61. Aitcheson SM, Frentiu FD, Hurn SE, Edwards K, Murray RZ. 2021. Skin wound healing: normal macrophage function and macrophage dysfunction in diabetic wounds. Molecules 26:4917. https://doi.org/10.3390/molecules26164917.
62. Ibberson CB, Jones CL, Singh S, Wise MC, Hart ME, Zurawski DV, Horswill AR. 2014. *Staphylococcus aureus* hyaluronidase is a CodY-regulated virulence factor. Infect Immun 82:4253–4264. https://doi.org/10.1128/IAI.01710-14.
63. Cohen TS, Takahashi V, Bonnell J, Tovchigrechko A, Chaerkady R, Yu W, Jones-Nelson O, Lee Y, Raja R, Hess S, Stover CK, Worthington JJ, Travis MA, Sellman BR. 2019. *Staphylococcus aureus* drives expansion of low-density neutrophils in diabetic mice. J Clin Invest 129:2133–2144. https://doi.org/10.1172/JCI126938.
64. Inouye M, Dashnow H, Raven LA, Schultz MB, Pope BJ, Tomita T, Zobel J, Holt KE. 2014. SRST2: rapid genomic surveillance for public health and hospital microbiology labs. Genome Med 6:90. https://doi.org/10.1186/s13073-014-0090-6.
65. Bankevich A, Nurk S, Antipov D, Gurevich AA, Dvorkin M, Kulikov AS, Lesin VM, Nikolenko SI, Pham S, Prjibelski AD, Pyshkin AV, Sirotkin AV, Vyahhi N, Tesler G, Alekseyev MA, Pevzner PA. 2012. SPAdes: a new genome assembly algorithm and its applications to single-cell sequencing. J Comput Biol 19:455–477. https://doi.org/10.1089/cmb.2012.0021.
66. Seemann T. 2014. Prokka: rapid prokaryotic genome annotation. Bioinformatics 30:2068–2069. https://doi.org/10.1093/bioinformatics/btu153.
67. Altschul SF, Gish W, Miller W, Myers EW, Lipman DJ. 1990. Basic local alignment search tool. J Mol Biol 215:403–410. https://doi.org/10.1016/S0022-2836(05)80360-2.
68. Johnson WL, Sohn MB, Taffner S, Chatterjee P, Dunman PM, Pecora N, Wozniak RAF. 2021. Genomics of Staphylococcus aureus ocular isolates. PLoS One 16:e0250975. https://doi.org/10.1371/journal.pone.0250975.
69. Vardi Y, Ying Z, Zhang C-H. 2001. Two-sample tests for growth curves under dependent right censoring. Biometrika 88:949–960. https://doi.org/10.1093/biomet/88.4.949.